

## SUPPORTING INFORMATION

### Wetting the Lock and Key Enthalpically Favours Polyelectrolytes Binding

Emeric Jeamet<sup>a</sup>, Jean Septavaux<sup>a</sup>, Alexandre Heloin<sup>a</sup>, Marion Donnier-Maréchal<sup>a</sup>, Mélissa Dumartin<sup>a</sup>, Benjamin Ourri<sup>a</sup>, Pradeep Mandal<sup>b</sup>, Ivan Huc<sup>b</sup>, Emmanuelle Bignon<sup>c,d</sup>, Elise Dumont<sup>\*c</sup>, Christophe Morell<sup>d</sup>, Jean-Patrick Francoia<sup>e</sup>, Florent Perret<sup>a</sup>, Laurent Vial<sup>\*a</sup> and Julien Leclaire<sup>\*a</sup>

<sup>a</sup>Institut de Chimie et Biochimie Moléculaires et Supramoléculaires, UMR 5246 CNRS - Université Claude Bernard Lyon1 - CPE Lyon, 43 Boulevard du 11 Novembre 1918, 69622 Villeurbanne Cedex, France.

<sup>b</sup>Institut de Chimie et Biologie des Membranes et des Nano-objets, UMR 5248 CNRS - Université de Bordeaux - IPB, 2 rue Escarpit, 33600 Pessac, France.

<sup>c</sup>Laboratoire de Chimie, UMR 5182 CNRS - Ecole Nationale Supérieure de Lyon - Université Claude Bernard Lyon 1 - CEA, 46 Allée d'Italie, 69364 Lyon Cedex 07, France.

<sup>d</sup>Institut des Sciences Analytiques, UMR 5280 CNRS - Université Claude Bernard Lyon 1 - Ecole Nationale Supérieure de Lyon, 5, rue de la Doua, 69100 Villeurbanne, France.

<sup>e</sup>Institut des Biomolécules Max Mousseron, UMR 5247 CNRS - Université de Montpellier - ENSCM, Place Eugène Bataillon, 34296 Montpellier Cedex 5, France.

\*elise.dumont@ens-lyon.fr; laurent.vial@univ-lyon1.fr; julien.leclaire@univ-lyon1.fr

1-	Potentiometric titrations .....	S2
2-	Crystallography .....	S3
3-	NMR complexation experiments.....	S3
4-	ITC titrations.....	S7
5-	Molecular Dynamics simulations .....	S10
6-	References.....	S13

## 1- Potentiometric titrations

All titrations were performed on a 702 SM Titrino automatic titrator. Solutions were prepared in 18 MΩ water. Experiments were performed in duplicate. Homemade Python scripts were used to fit experimental data and are available on simple request.

*Preparation of the titrating solution:* A ~0.05 M sodium hydroxide solution was prepared by dissolving sodium hydroxide pellets in pure water. The solution was degassed by ultrasounds and nitrogen was bubbled through the solution for 30 minutes. The exact concentration of the NaOH solution was subsequently obtained by titrating a solution of potassium phthalate. Final concentration: 45.59 mM.

*Blank titration:* 1 mL of a ~ 0.1M HCl solution was titrated with the calibrated sodium hydroxide solution to obtain the exact concentration of the H<sup>+</sup> ions. Final concentration: 90.7 mM.

*Macrocycle titration:* 11.85 mg of **1<sub>4</sub>** were dissolved in 5 mL of pure water, and 1 mL of the above HCl solution was added to acidify the mixture. As **1<sub>4</sub>** was not soluble in water at low pH, the titration method was modified in order to reach pH stabilization after each addition. During the titration, **1<sub>4</sub>** was completely soluble above pH = 5.

*Data treatment:* In the first place, the concentration of H<sup>+</sup> ions was calculated for each experimental point of the blank titration using equation (1):

$$[H^+] = ([H^+]_0 - [OH^-] \times V) / (V + V_0) \quad (1)$$

Where [H<sup>+</sup>]<sub>0</sub> is the concentration of the titrated HCl solution, [OH<sup>-</sup>] the concentration of the titrated NaOH solution, V<sub>0</sub> the initial volume of the sample, and V the volume of added base during the blank titration. Then the activity coefficient γ that accounts for the non-ideal behavior of ions was calculated by fitting equation (2) to the data [H<sup>+</sup>] = f(pH) obtained from the blank titration.

$$[H^+] = (10^{-pH} - 10^{pH-pK_w}) / \gamma \quad (2)$$

The corrected acidity function [H<sup>+</sup>]<sub>c</sub> = f(pH) of the blank could then be calculated from equation (2) and γ. The acidity function [H<sup>+</sup>]**1<sub>4</sub>** = f(V) in presence of **1<sub>4</sub>** could be obtained from equation (3), and the concentration of acidic groups C<sub>p</sub> could be calculated from equation (4), where N<sub>p</sub> is the quantity of acidic groups (assuming that **1<sub>4</sub>** bears 8 acidic groups). As the pH was known for each value of V during the titration, [H<sup>+</sup>]**1<sub>4</sub>** = f(pH) and C<sub>p</sub> = f(pH) could be trivially extracted.

$$[H^+]\mathbf{1}_4 = ([OH^-] \times V) / (V_0 + V) \quad (3)$$

$$C_p = N_p / (V_0 + V) \quad (4)$$

Finally, the protonation degree θ = f(pH) can be calculated from equation (5). At pH 7.4, we obtained the following protonation degrees: -0.8 % and -0.09 %.

$$\theta = (C_p - [H^+]_c - [H^+]\mathbf{1}_4) / C_p \quad (5)$$

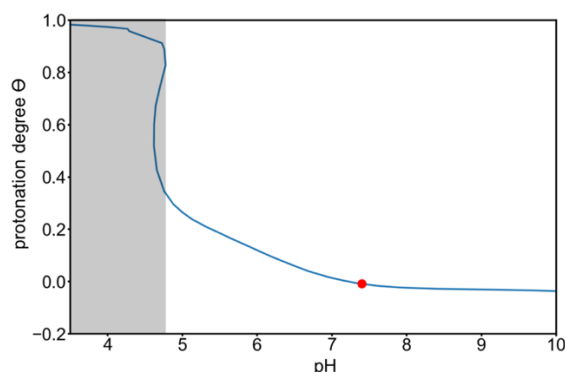


**Fig. S1** Protonation degree Θ versus pH curve for dyn[4]arene **1<sub>4</sub>** in deionized water. The red dot and the grey rectangle highlight pH = 7.4 and the low-solubility region of the macrocycle, respectively.

## 2- Crystallography

X-ray quality crystals were obtained using hanging drop vapor-diffusion method in 24-well Linbro-style plates. The drops were equilibrated against 500  $\mu$ l of crystallization reagent (1.2 M Ammonium sulfate, 0.1 M HEPES (pH 7.5), 2 % w/v Polyethylene glycol 400) in the reservoir. X-ray diffraction data were collected using Rigaku FRX micro-focus rotating anode (2.9kW) and PILATUS 200K hybrid pixel detector, at the IECB X-ray facility (UMS 3033). Diffraction data were processed using the CrysAlisPro package. The structure was solved with *Shelxt*<sup>1</sup> and refined by full-matrix least-squares method on  $F^2$  with *Shelxl-2014*<sup>2</sup> within the *Olex2* suite.<sup>3</sup>

Non-hydrogen atoms for the host and guest molecule were refined with anisotropic displacement parameters. Hydrogen atoms were added for the host and guest in idealized positions using HFIX and refined with riding model. For few of the solvent molecules, positions of hydrogen were determined. DFIX, DELU, SIMU and ISOR instructions were used in order to model displacement parameters and geometry of molecules. FVAR function was used during refinement of occupancy factors of disordered parts. The final cif files were examined using IUCR's checkcif algorithm. The B-level alerts (PLAT306\_ALERT\_2\_B Isolated Oxygen Atom (H-atoms Missing?)) corresponded to hydration water molecules. The thermal nature of water molecules and the level of apparent electron densities assured their modeling.

Atomic coordinates and structure factors for the crystal structure of *rac*-Lys-NH<sub>2</sub> **1**<sub>4</sub> have been deposited in the Cambridge Crystallographic Data Centre (CCDC) with accession code 1554746 respectively. These data are available free of charge upon request ([www.ccdc.cam.ac.uk/](http://www.ccdc.cam.ac.uk/)).

## 3- NMR complexation experiments

<sup>1</sup>H NMR spectra were recorded in heavy water at pH 7.4 on a spectrometer operating at 300 MHz. 3-(trimethylsilyl)propionate-2,2,3,3-d<sub>4</sub> signal was used as internal standard.

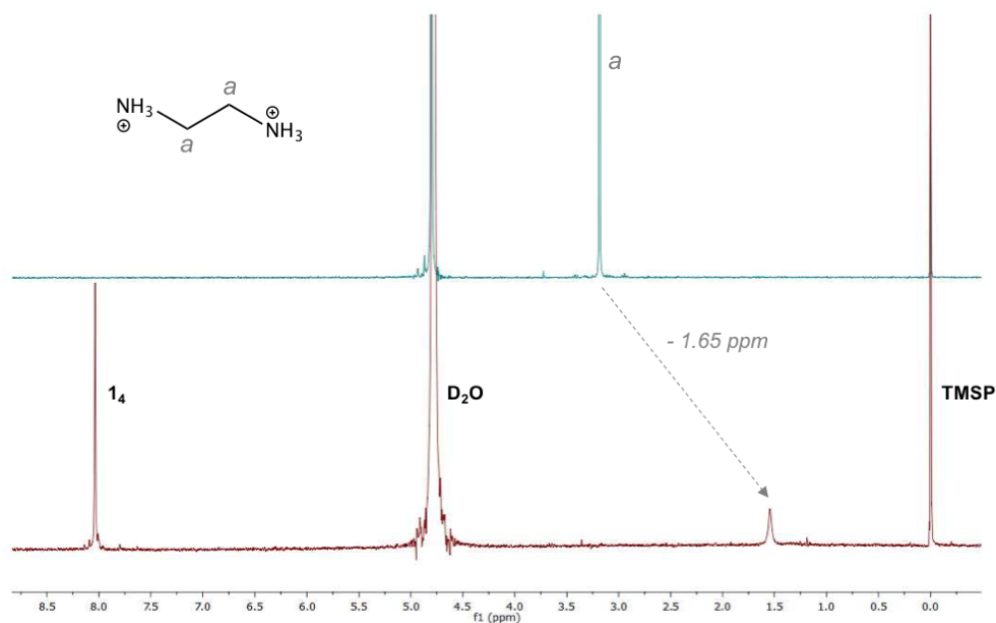


**Fig. S2** <sup>1</sup>H NMR spectrum of 1,2-diaminoethane **2** (top), and its corresponding 1:1 complex with dyn[4]arene **1**<sub>4</sub> (below).

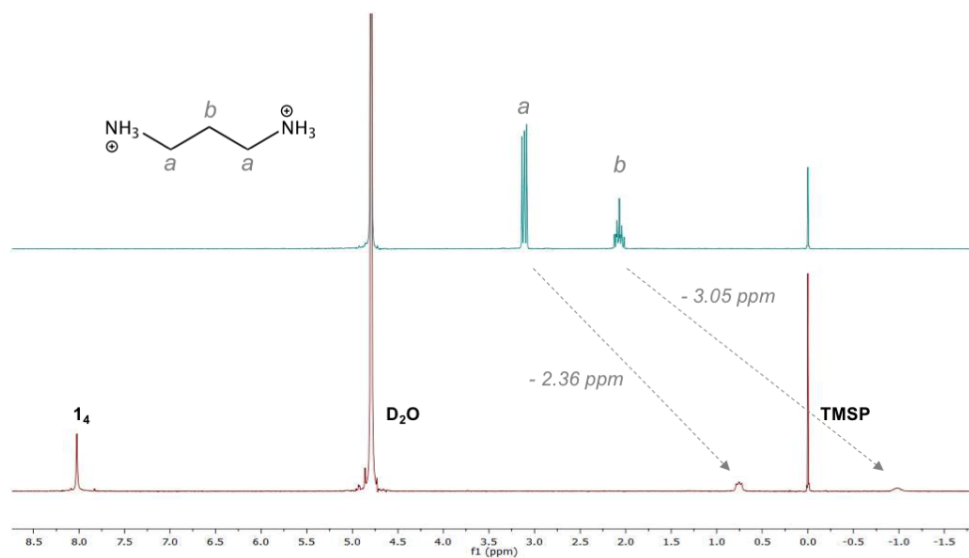


**Fig. S3** <sup>1</sup>H NMR spectrum of 1,3-diaminopropane **3** (*top*), and its corresponding 1:1 complex with dyn[4]arene **14** (*below*).

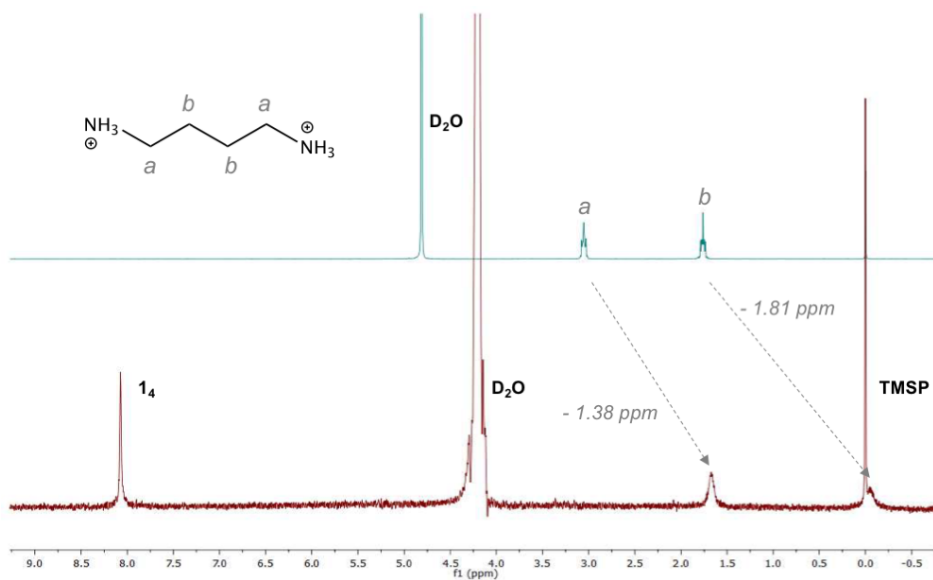


**Fig. S4** <sup>1</sup>H NMR spectrum of 1,4-diaminobutane **4** (*top*), and its corresponding 1:1 complex with dyn[4]arene **14** (*below*).

\*the spectrum of **4**  $\subset$  **14** was actually recorded at 353 K in order to obtain signals for the guest that were sharp enough to be distinguished from the baseline.

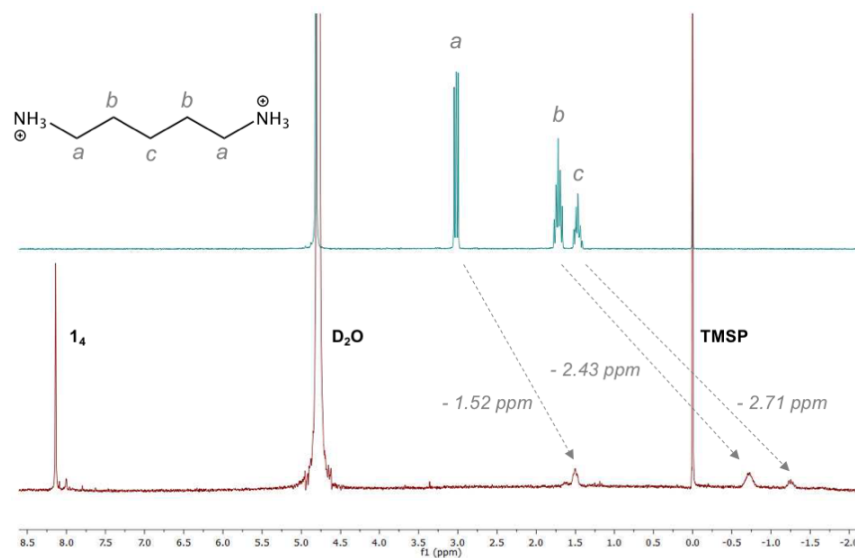


**Fig. S5**  $^1\text{H}$  NMR spectrum of 1,5-diaminopentane **5** (top), and its corresponding 1:1 complex with dyn[4]arene **14** (below).

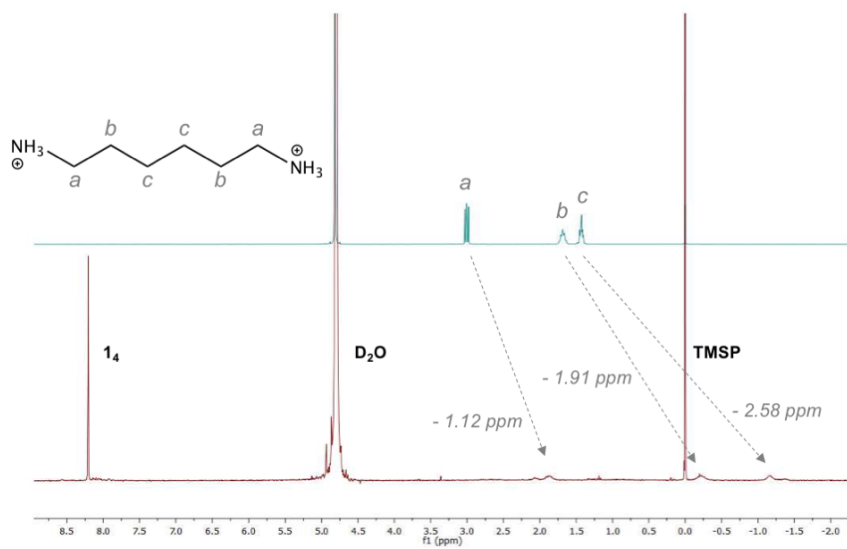


**Fig. S6**  $^1\text{H}$  NMR spectrum of 1,6-diaminohexane **6** (top), and its corresponding 1:1 complex with dyn[4]arene **14** (below).

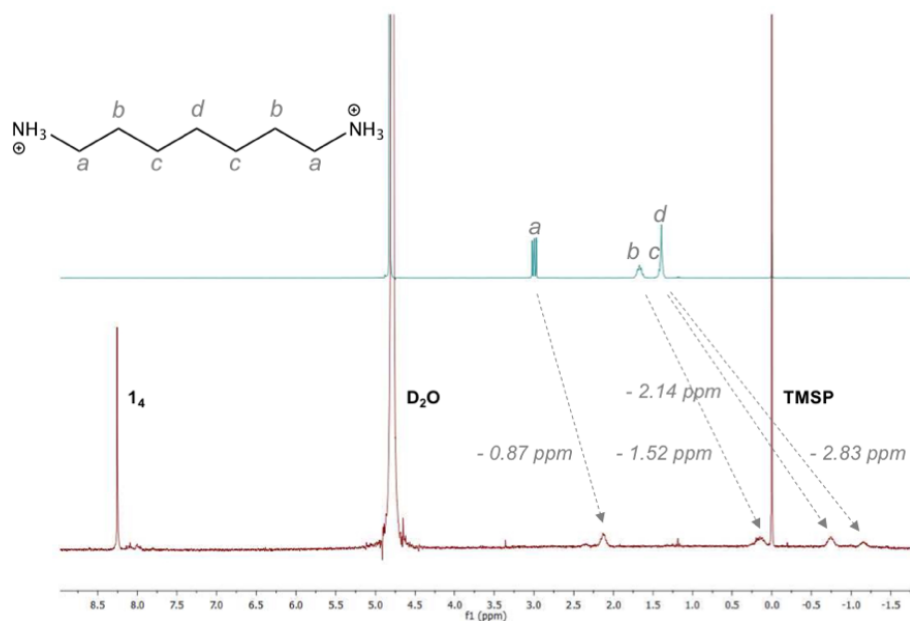


**Fig. S7** <sup>1</sup>H NMR spectrum of 1,7-diaminoheptane **7** (top), and its corresponding 1:1 complex with dyn[4]arene **14** (below).

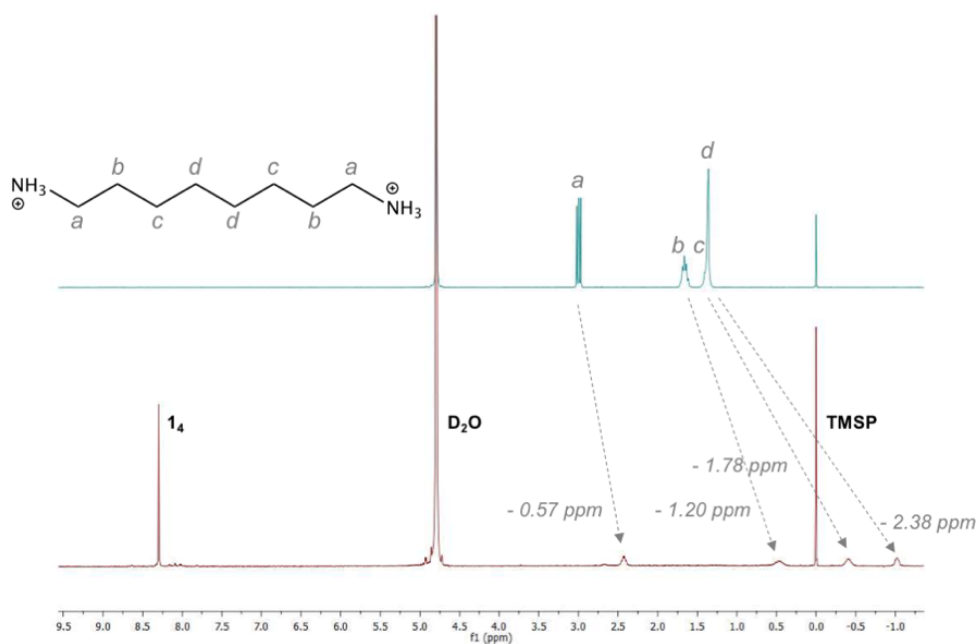


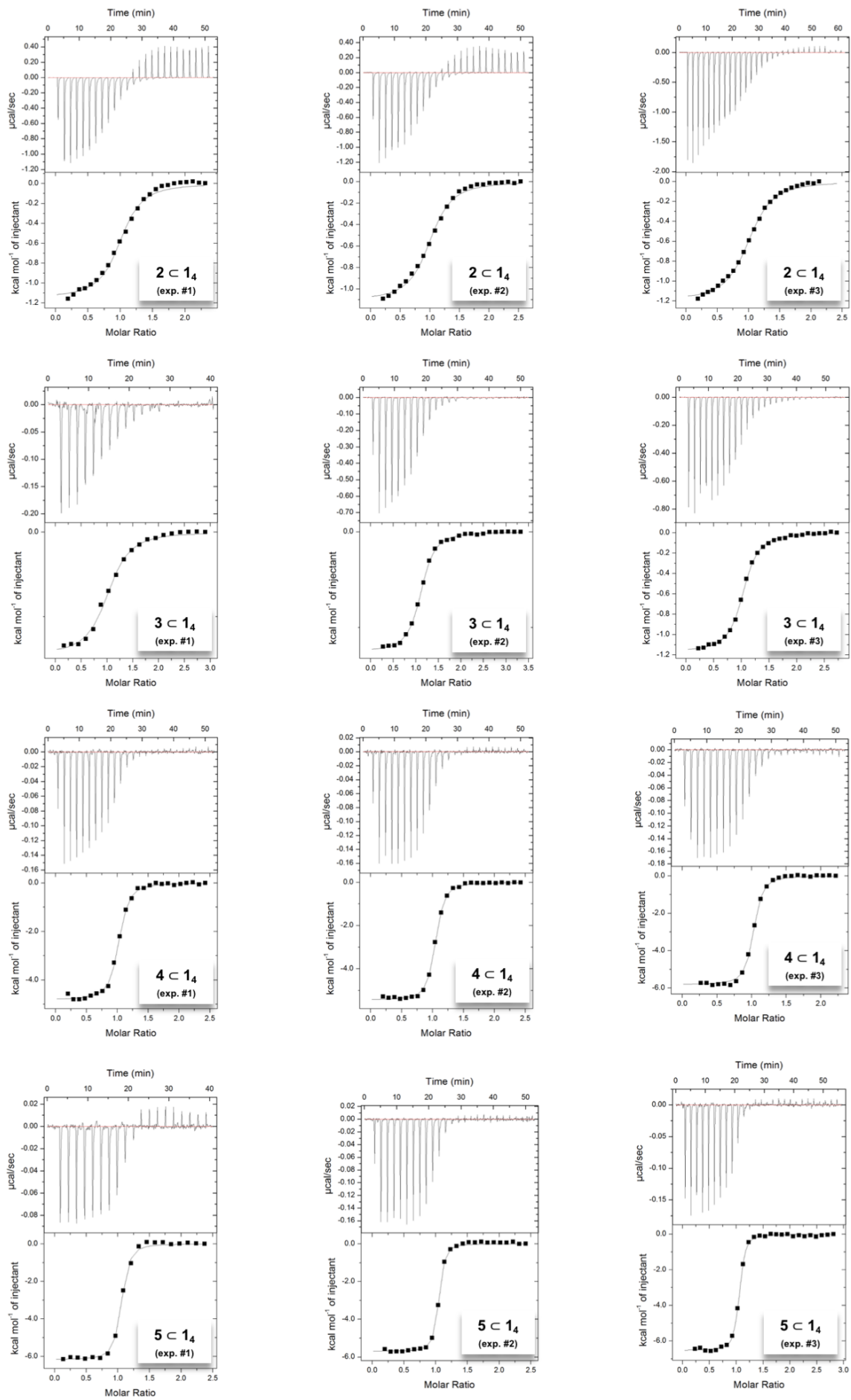
**Fig. S8** <sup>1</sup>H NMR spectrum of 1,8-diaminooctane **8** (top), and its corresponding 1:1 complex with dyn[4]arene **14** (below).

#### 4- ITC titrations

Isothermal Titration Calorimetry (ITC) experiments were performed at 298 K. In a standard experiment, the host solution in Tris buffer pH 7.4 (200 mM) was placed into the calorimeter cell (200  $\mu$ l) and successive aliquots of guest solution were added via a computer-automated injector at 2 min intervals. Heat changes were recorded after each addition. The first injection was discarded from each dataset to remove the effect of guest diffusion across the syringe tip during the equilibration process. Thermodynamic parameters were obtained from the 1:1 binding model of the MicroCal ITC Origin software. Each experiment was performed in triplicate.

Complex	Exp. #	[Host]	[Guest]	K (10 <sup>7</sup> )	$\Delta$ K	$\Delta$ K/K	Delta H	$\Delta$ delta H	Delta S	N	c parameter
<b>2</b> $\subset$ <b>1<sub>4</sub></b>	1	1,2	20	0,00307	0,000359	0,117	-1037	15,48	17,1	0,8	27
	2	1,1	20	0,00332	0,000457	0,138	-951,8	17,09	17,5	0,8	29
	3	1,3	20	0,00283	0,000244	0,086	-1028	10,59	16,9	0,9	33
<b>3</b> $\subset$ <b>1<sub>4</sub></b>	1	0,07	1	0,03	0,00370	0,123	-1449	26,42	20,2	0,8	17
	2	0,30	7,5	0,0153	0,00077	0,050	-1251	7,23	19,5	0,7	33
	3	0,40	7,5	0,0127	0,00061	0,048	-1173	6,369	19,4	0,9	45
<b>4</b> $\subset$ <b>1<sub>4</sub></b>	1	0,02	0,3	0,865	0,083	0,095	-4811	34,17	15,6	0,9	131
	2	0,02	0,3	1,24	0,088	0,071	-5444	24,91	14,2	0,9	193
	3	0,02	0,3	1,04	0,107	0,103	-6112	45,66	11,6	1,0	183
<b>5</b> $\subset$ <b>1<sub>4</sub></b>	1	0,009	0,1	3,32	0,531	0,160	-6171	52,12	13,2	1,0	283
	2	0,016	0,3	3,64	0,388	0,107	-5691	26,45	15,5	0,9	534
	3	0,016	0,3	2,36	0,202	0,086	-6530	30,51	11,8	0,9	316
<b>6</b> $\subset$ <b>1<sub>4</sub></b>	1	0,02	0,3	3,38	0,294	0,083	-6580	23,09	13,2	1,1	570
	2	0,02	0,3	5,19	0,432	0,126	-5937	34,59	14,2	1,0	570
	3	0,01	0,1	4,04	0,261	0,065	-6557	20,01	12,8	1,1	458
<b>7</b> $\subset$ <b>1<sub>4</sub></b>	1	0,02	0,3	5,31	1,12	0,211	-7482	60,25	10,2	0,9	892
	2	0,01	0,2	5,27	1,290	0,245	-7616	66,8	9,78	1,0	557
	3	0,01	0,2	2,01	0,324	0,161	-7440	67,97	8,46	1,1	320
<b>8</b> $\subset$ <b>1<sub>4</sub></b>	1	0,008	0,1	2,02	0,312	0,154	-9257	94,28	2,37	0,9	147
	2	0,018	0,3	1,62	0,149	0,092	-8392	45,04	4,84	0,9	260
	3	0,018	0,2	2,68	0,202	0,075	-9027	44,97	3,71	0,8	390

**Table S1** Experimental conditions and collected data from ITC titrations of dyn[4]arene **1<sub>4</sub>** with guest **2-8** : concentrations in mmol.L<sup>-1</sup>, association constants in M<sup>-1</sup>, enthalpies in cal.mol<sup>-1</sup>, and entropies in cal.mol<sup>-1</sup>.deg<sup>-1</sup>. The Wiseman “c” parameter (which is the product of the stoichiometry, receptor concentration and binding constant) is optimal in the so-called “experimental window” of c values of 10 to 1000, see ref. 5.



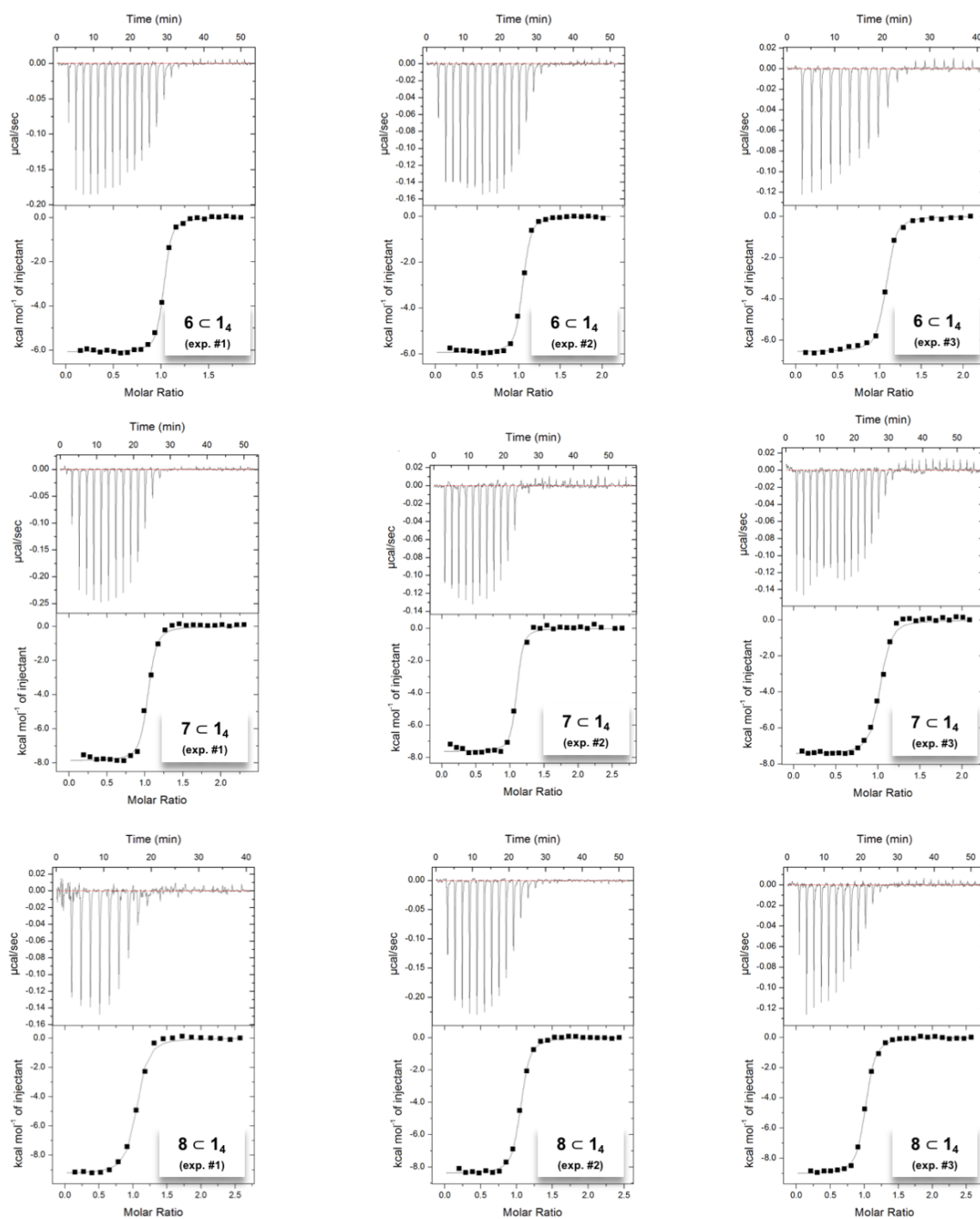


**Fig. S9** ITC data obtained for the titration of dyn[4]arene **14** with guest **2-8** in the conditions described in Table S1. The upper panel presents raw differential heating power over time, and the lower panel displays the integrated heat per addition over molar ratio between the guest and **14**. Solid lines correspond to the best fit using the 1:1 binding model within the Origin software.

## 5- Molecular Dynamics simulations

All molecular dynamic simulations and post-processing were performed with the Amber 12 Molecular Dynamics software package. The force-field parameters were taken from parm99, while the parameters for the cage were generated using the generalized AMBER force field GAFF. Each compound was previously build using the Spartan software and their geometries were optimized with the Gaussian09 suite of programs software using density functional theory at the B3LYP level of theory with the 6-31G(d,p) basis set. The different parameters were generated with antechamber and parmcheck subprograms, and atom point charges were computed using the RESP proto-col. The guest was inserted at specific position around the host using the xleap module. Ammonium cations ( $\text{NH}_4^+$ ) were added in order to neutralize the systems, which were immersed in a truncated octahedral water TIP3P water box containing  $\sim 8000$  water molecules (10 Å buffer). Each system was first minimized in a 5000 steps simulation, including 2500 steps of steepest descent. Then, a thermalization step was performed to heat each system from 0 to 300 K in 30 ps. The temperature was kept constant during the following steps using Langevin thermostat with a collision frequency  $\gamma$  of  $1 \text{ ps}^{-1}$ . A 100 ps equilibration run was performed in NPT conditions. Finally, a 100 ns production was executed with constant pressure. After all dynamic molecular simulations, a cluster analysis was performed using the cpptraj module of AMBER, and thermodynamic parameters were extracted using the MM/GBSA method with the internal and external dielectric constants set to 1 and 80, respectively. The salt concentration was assigned to 0.1M. Trajectories were visualized with the VMD software.<sup>4</sup>

### 5.1. Dynamic molecular post processing

#### 5.1.1. Cluster analysis

After all dynamic molecular simulations, cluster analyses were performed to provide the ten structures most present during the calculation. The distribution (A to J) of these conformations for each simulation was shown in the following. For the most balanced distribution (complex **8 c 1<sub>4</sub>**), we provide below cartoon representations showing the superimposed structure of the most populated structure (A, prevalence 22%) vs. the three following most populated conformers (B, C, D).

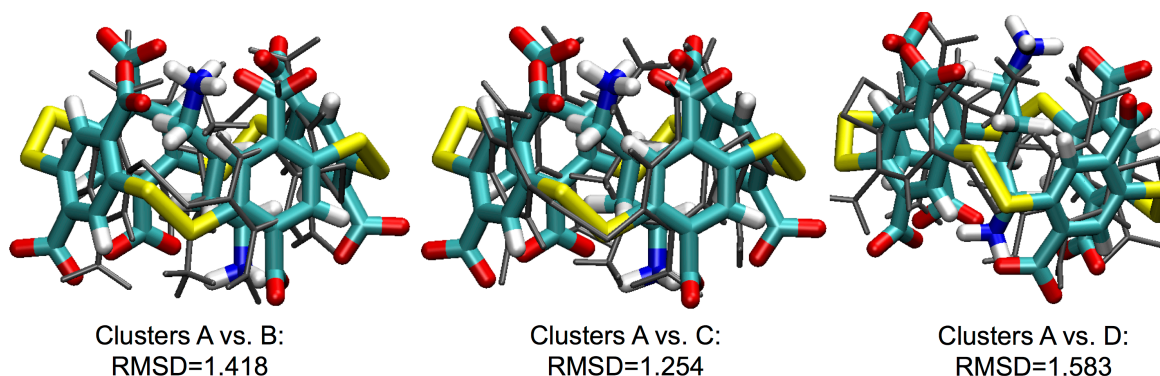


**Fig. S10** Cartoon representations of the three conformers B, C and D identified by cluster analysis superimposed with the cluster A (prevalence 22%) for guest **4** interacting with the host **1<sub>4</sub>** (third line of Table 3). The structures differ by a slight translation of the guest with respect to the carboxylates and changes of conformation of the disulfide bridges.

#### 5.1.1.1. Host **1<sub>4</sub>** alone

	A (%)	B (%)	C (%)	D (%)	E (%)	F (%)	G (%)	H (%)	I (%)	J (%)
<b>(pR)<sub>4</sub></b>	39	36	12	12	1	/	/	/	/	/
<b>(pR<sub>3</sub>pS)</b>	61	36	2	/	/	/	/	/	/	/
<b>(pRpS)<sub>2</sub></b>	31	27	14	11	6	5	3	3	/	/
<b>(pR)<sub>2</sub>(pS)<sub>2</sub></b>	90	10	/	/	/	/	/	/	/	/

**Table S2** Conformation repartition of **1<sub>4</sub>** structures after cluster processing.

### 5.1.1.2. Complexes between **1<sub>4</sub>** and various $\alpha$ - $\omega$ -alkyl-diamines

	A (%)	B (%)	C (%)	D (%)	E (%)	F (%)	G (%)	H (%)	I (%)	J (%)
<b>n=2</b>	33	23	12	12	8	6	3	2	2	/
<b>n=3</b>	25	18	17	17	14	5	1	1	1	/
<b>n=4</b>	22	20	19	12	12	7	4	1	1	/
<b>n=5</b>	30	25	23	19	1	1	/	/	/	/
<b>n=6</b>	29	23	22	22	3	1	/	/	/	/
<b>n=7</b>	40	21	18	17	1	1	1	1	/	/
<b>n=8</b>	66	18	10	2	2	1	1	1	/	/

**Table S3** Conformation repartition of complex **1<sub>4</sub>**/ $\alpha$ - $\omega$ -alkyl-diamine structures after cluster processing.

### 5.1.2. Convergence of the MM/GBSA post-processing.

Our dynamics were post-processed for the last 100 ns of trajectories to extract free energies of binding. We report here the MM/GBSA values of free binding energy (in kcal.mol<sup>-1</sup>) calculated along each 10 ns segment. They reflect a rapid convergence within the first 10 ns of simulation.

	0-10 ns	10-20 ns	20-30 ns	30-40 ns	40-50 ns	50-60 ns	60-70 ns	70-80 ns	80-90 ns	90-100 ns
<b>n=2</b>	-28.5±3.4	-28.6±4.1	-28.2±4.0	-28.1±3.9	-27.9±4.3	-27.8±4.3	-27.6±4.6	-27.7±4.6	-27.8±4.4	-27.8±4.4
<b>n=3</b>	-30.4±4.6	-30.4±4.7	-30.4±5.5	-30.4±4.3	-30.5±4.6	-30.5±4.4	-30.5±4.6	-30.6±4.5	-30.7±4.5	-30.3±3.8
<b>n=4</b>	-34.3±4.4	-34.2±4.8	-34.4±4.3	-34.4±4.0	-34.3±4.0	-34.4±3.9	-34.5±3.7	-34.3±4.3	-34.1±4.7	-34.1±5.5
<b>n=5</b>	-35.4±4.9	-35.6±5.3	-35.8±4.9	-35.5±6.0	-35.5±5.6	-35.5±5.3	-35.2±6.2	-35.3±6.0	-35.3±5.8	-35.8±5.8
<b>n=6</b>	-36.6±3.6	-36.5±3.6	-36.4±4.9	-35.8±6.8	-36.0±6.4	-36.1±6.0	-36.1±6.0	-36.1±6.0	-36.2±6.0	-36.3±3.6
<b>n=7</b>	-35.6±5.1	-35.6±5.2	-35.6±5.3	-35.8±4.4	-36.0±3.9	-36.0±3.0	-36.0±3.0	-36.3±2.8	-36.3±2.8	-36.5±2.8
<b>n=8</b>	-37.5±5.8	-37.6±5.7	-37.4±5.6	-37.4±5.5	-37.0±6.6	-37.0±6.7	-37.0±6.6	-37.0±6.6	-37.5±6.6	-38.4±3.4

**Table S4** MM/GBSA binding free energies evaluated along 10 segments of 10ns of the MD trajectories.

## 5.2. Solvation pictures of the complexes between host **1<sub>4</sub>** and guests **2-8**

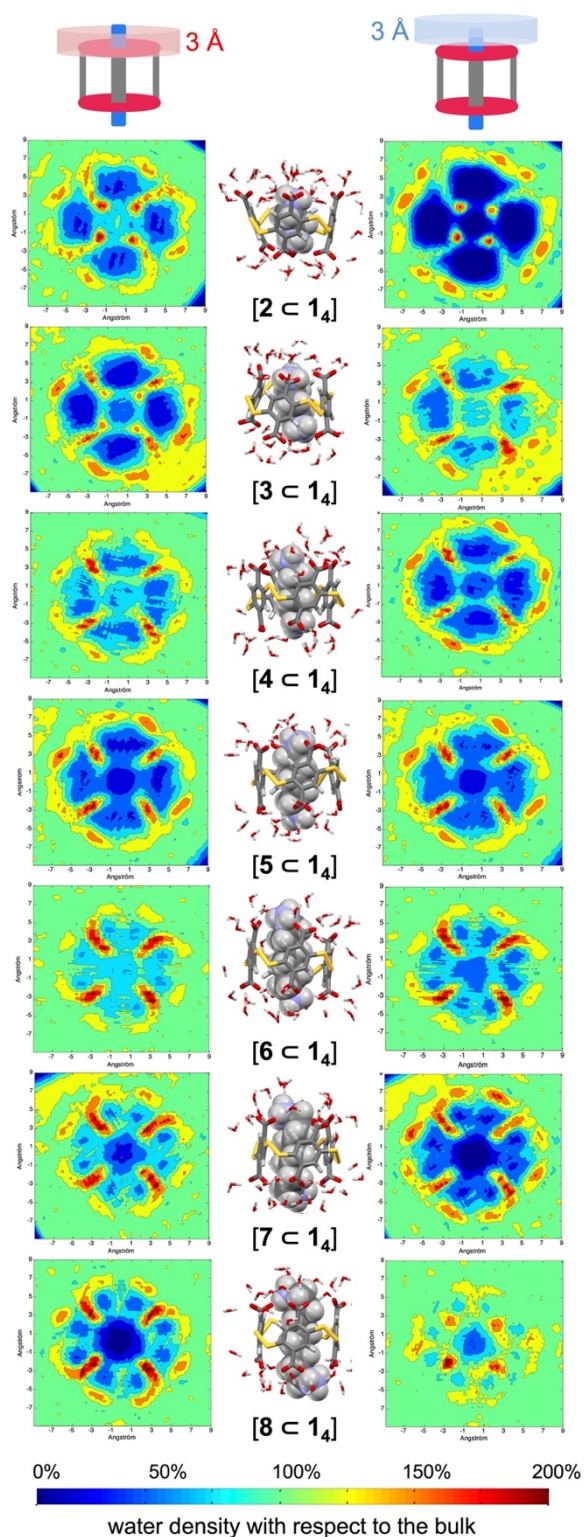


**Fig. S11** Time-averaged density of water molecules around the complexes formed between the dyn[4]arene **1<sub>4</sub>** and  $\alpha,\omega$ -alkyldiammonium ions **2-8** from the MD trajectories. Left and right maps correspond to the first solvation layers of the carboxylate rims and the ammonium heads, respectively. Corresponding snapshots from the MD trajectories are displayed in the middle. Bottom: increased water density scale from dark blue (0 %) to dark red (200 %), with respect to the bulk (green) as the average value (100 %).

## 6- References

---

- 1 G. M. Sheldrick, *Acta Crystallogr., Sect. A*, 2015, **71**, 3.
- 2 G. M. Sheldrick, *Acta Crystallogr., Sect. C*, 2015, **71**, 3.
- 3 O. V. Dolomanov, L. J. Bourhis, R. J. Gildea, J. A. K Howard, H. Puschmann, *Appl. Cryst.*, 2009, **42**, 339.
- 4 W. Humphrey, A. Dalke, K. Schulten, *J. Mol. Graphics*, 1996, **14**, 33.
- 5 M. R. Duff, Jr., J. Grubbs, E. E. Howell *J. Vis. Exp.* 2011, **55**, 2796.